Impact of the wave/wind induced oscillations on the power performance of the WindFloat wind turbine

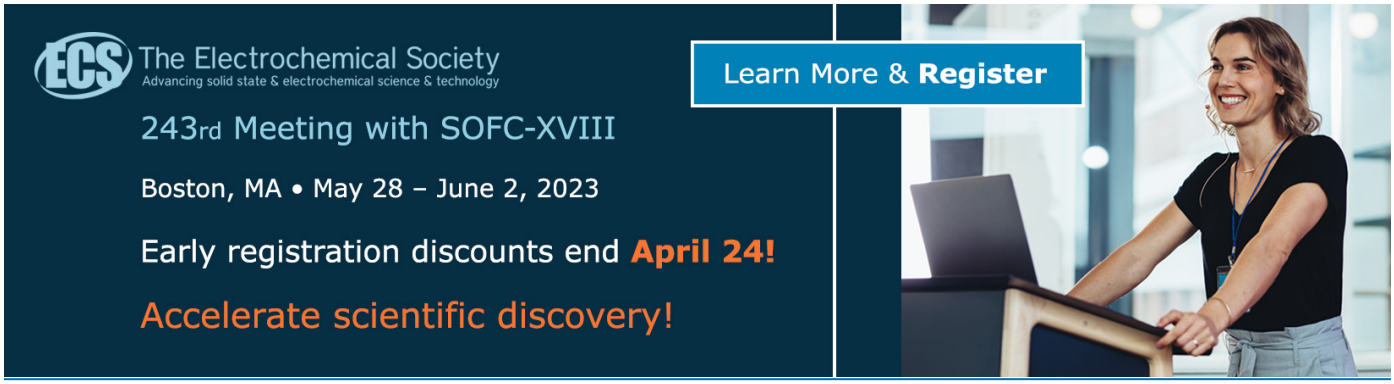

Impact of the wave/wind induced oscillations on the power performance of the WindFloat wind turbine

A Couto[1], P. Justino[1], T Simões[1] and A Estanqueiro[1]

[1] Unidade de Energias Renováveis e Eficiência Energética, Laboratório Nacional de Energia e Geologia - LNEG, I.P., Lisboa, Portugal

antonio.couto@lneg.pt, paulo.justino@lneg.pt, teresa.simoes@lneg.pt, ana.estanqueiro@lneg.pt

Abstract. The main objective of this work is the characterization of the wave/wind induced oscillations on the power performance of the wind turbine operating on a WindFloat floating system. To assess the potential impact on the wind turbine power performance induced by these oscillations, the nacelle movements of the WindFloat wind turbine were monitored using accelerometer sensors synchronized with : 1) metocean data measured with a buoy; 2) wind turbine power data installed in the WindFloat floating system; and 3) wind speed data gathered from a nacelle-mounted LiDAR. Based on this data, a clustering analysis approach is proposed. No meaningful relationship between the ocean parameters and the nacelle movements or the wind power production could be established. The obtained results suggest that the dynamic adaptation of the drive train (mainly due to wind turbine torque control) to a fast oscillating (primary energy) moving force is the source of the largest oscillations in the nacelle of the WindFloat wind turbine. Nevertheless, results suggest that the wind/wave induced oscillations and their impact on the power performance of the WindFloat wind turbine is low considering its nominal capacity. Outcomes of this work were extremely relevant to demonstrate the stability of the WindFloat system, and, consequently, also important for the development of the floating wind offshore industry (and other technologies).

1. Introduction

Offshore wind energy is a key contributor to the EU's targets for the decarbonization of the electrical power systems. The offshore renewable energy strategy established within the scope of the European Green Deal defines a minimum of 60 GW of wind power installed until 2030 [1]. In fact, the offshore wind resource potential in Europe is very significant. Currently, the growth of this sector has been mainly using bottom fixed technology, limiting installations to depths of less than 60 meters. This is justified by the high costs of the floating technology and its immature state of development that makes deployment in deeper waters a very challenging and expensive process. Thus, the inability to exploit the wind potential of the deeper regions can limit the growth of the offshore wind industry. This issue is relevant in countries such as Portugal, where the highest offshore wind potential was identified over deeper waters.

In this sense, new solutions, especially for deep offshore regions, are needed and floating wind turbines, such as WindFloat or Hywind systems, can overcome the previously indicated limitations and be an economically sustainable technology in the near future [2,3]. More benefits are expected from the transition to floating wind turbines: mitigates potential land-use conflicts, minimizes visual impacts associated with shallow water and onshore technologies, and highest wind resources. Some

floaters allow quayside mounting which enables simplifying the installation procedures and the use of specialized vessels is not required [2].

Inspired by industries such as oil and gas, different platform configurations for floating offshore wind turbines were developed. Although with different configurations, floating platforms can be classified into three main concepts: semi-submersibles, spar buoys and tension-leg platforms [3]. From a technical point of view, floating wind technology needs to prove its viability to be exploited on large-scale. Specifically, this technology needs to prove that there are no deficits in the energy performance of the wind turbine due to potential effects induced by wind/wave in the system when compared to onshore or offshore fixed to bottom-fixed technologies [4]. To prove the reliability of the floating systems two main aspects must be scrutinized: 1) the influence of the wind turbine on the floater; and 2) the influence of the floater motion induced by waves on the wind turbine performance [5,6].

One of the main challenges in developing a floating wind turbine system is to ensure the turbine itself is stable and aerodynamically efficient [5,7]. In this sense, several experimental studies using scaled floating turbines in wave tank tests [8–10] or computational fluid dynamic (CFD) models are available but they are commonly limited to investigating the dynamic response of the floating structure and not the power performance of the wind turbine [7,11,12]. The impact of the pitching motion of the platform on the aerodynamic response as well as the wake behaviour of the offshore wind turbine response was analysed by Tran et al.[13], Lei et al. [14] and Wen et al. [15] using CFD simulations. Pitching motion can have a positive significant impact with an increase in power output observed. In the work presented by Nejad et al. [16], the authors highlighted that the effect of wave-induced motions may not be as significant as the wind loading on the drivetrain responses, particularly in larger turbines. However, the limited experience with floating wind turbines requires further research. Using simulation and analytic approaches, for instance, Johlas et al. [17] examined the impact on the power values due to the platform and rotor displacements under extreme conditions. The authors concluded that the rotor displacements do not significantly affect the average power values extracted from the floating wind turbine. Using a tension-leg platform in a wave tank, Sant et al. [9] identified a dependency of power generation from the ocean conditions observed. Indeed, the power performance characteristics present slight deviations in the time-averaged power coefficients when compared with those obtained for a fixed wind turbine. Therefore, the authors pointed out that it is expected to be more challenging to define the wind turbine power curve installed on a floating structure due to the wave dependency.

This work focuses on the WindFloat (WF) system. The WindFloat is a semi-submersible platform, which combines a wind turbine and a floater [5,8,18]. The WindFloat system has been modelled, tested and validated in scale model and wave tank tests and demonstrated acceptable static and dynamic motions for the operation of large wind turbines [5]. In order to improve the design of future floating structures and to demonstrate the economic sustainability of this technology, also the impact of the wave/wind induced oscillations on the power production of a floating wind turbine must be addressed. The results for the WindFloat system in wave tank tests showed that for a wave induced with 4 m and a wind speed of 12 m/s, due to a resonance response between wind turbine control system and the platform a slight decrease in the power output may occur [8]. This reduced impact can be partially explained by the high dynamic stability of the WindFloat platform. The stability is achieved by: 1) the heave plates located at the base of the three columns which provide buoyancy to support turbine from the water plane inertia; and 2) an active water ballast system that compensates changes in mean wind velocity and direction keeping the tower vertical to maintain the turbine performance [5,18]. Nevertheless, the challenges associated with the operation of floating wind turbines in real offshore environment [4], where the wind/wave induced effects on the floating foundation of the wind turbine present a six degrees of freedom oscillations (yaw, pitch, roll, surge and sway), can induce an impact higher than the one observed in the controlled experimental reduced scale studies. Therefore, these results required validation in a real environment, where the floating wind turbines are exposed to stochastic and severe weather/ocean conditions that can influence their performance. For the specific case of WindFloat, this validation was performed during the European DEMOWFloat project that ended with very successful results in 2016, which were the origin of the

upscaling of this floater [19]. As highlighted in [12], the information regarding real environment campaigns is scarce and limited due to confidentiality reasons.
The goal of this work is to present a methodology to assess the impact of the wave/wind induced oscillations on the wind turbine power curve performance operating at WindFloat system by using real data gathered during the DEMOWFloat project. As a side effect, this assessment contributes to the development and adaptation of the international standards for wind turbine's power curve characterization for the specific case of floating wind turbines. The results of this work, obtained in a real operating environment, are extremely relevant to demonstrate the stability of the WindFloat system, and consequently, are crucial for the development of the wind offshore floating industry (and other technologies).

2. Data

This work uses data from the experimental campaign from the DEMOWFloat project. This campaign was held in the Northwest region of Portugal and deployed the following systems: 1) a buoy from Axys Technologies with a Vindicator *Light* Detection and Ranging (*LiDAR*) and with equipment to obtain ocean data; 2) a wind turbine model Vestas V80; and 3) a nacelle-mounted LiDAR (hereafter designated as NL) located on the top of the wind turbine. The geographical location of the different measuring systems under analysis is presented in Figure 1, while the data coverage considered in this work is presented in Table 1. It should be noted that all data were collected following the international standard for wind turbine power performance assessment [20].

Table 1. Identification of the measurement systems available and their data coverage.

Measurement system	Data coverage
Buoy with floating LIDAR (FL)	30.09.2014 to 31.04.2015
Nacelle-mounted LIDAR (NL)	20.06.2014 to 31.04.2015
WindFloat with wind turbine, accelerometers and nacelle anemometry	01.01.2014 to 20.04.2015

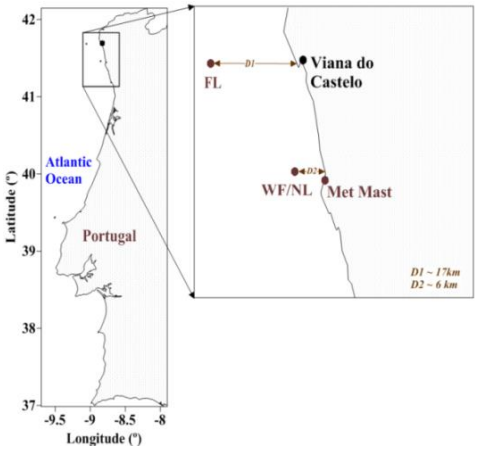

Figure 1. Measurement systems location.

2.1. Buoy with a floating LIDAR data

The buoy was located in an offshore region near Viana do Castelo. For this specific work, only ocean data were used from this system. The most relevant ocean parameters available are: significant wave height (m), maximum wave height (m), peak period (s), mean wave direction (degrees), significant period (s), average wave height (m), average wave period (s), peak period read method (s), and significant wave height spectral moment (m). Since each record of wave data corresponds to an average of the previous 30 minutes, the last wave record was repeated for two preceding records of 10-minute enabling to obtain ocean data for the same time steps of the remaining measurement systems. Based on the significant wave height (H_s) and peak period (T_p), it was possible to calculate the wave steepness for a shallow water approximation, Equation (1).

$$Steepness = \frac{2\pi H_S}{g T_P^2} \quad (1)$$

where, g is the gravitational acceleration (m/s^2). This parameter is related to the slope of the waves.

2.2. Data gathered from wind turbine

A common onshore Vestas V80 wind turbine with a rated capacity of 2.0 MW was installed on the WindFloat floater. From the wind turbine, it was possible to obtain the following data: active power generated, status codes from wind turbine and the wind rotor's revolutions per minute (RPM). The nacelle anemometry provides the wind speed at wind turbine location. The data were gathered in 10 minute' bins from which the respective standard deviation, maximum and minimum values were also collected. Additionally, nine accelerometers, six of them dedicated to monitoring the accelerations from the wind turbine nacelle were installed. The sampling rate of these sensors was 50 Hz and the data are recorded in individual files every 10 minutes.

2.3. Nacelle-mounted LiDAR data

The two-beam Wind Iris LIDAR model was installed on top of the wind turbine's nacelle. This system uses pulsed LIDAR technology which enables the measurement of the horizontal upwind wind speed from a distance ranging from 80 to 440 meters, with a spatial distance of 40 meters amid two measurement distances. To accomplish with the existing international standards, only the upwind distance of 200m (2.5 times the diameter of the wind turbine) was considered in this work.

3. Methodology

To ensure the evaluation of the wind turbine's power curve during normal operation as required by the actual power performance standards it is proposed a new filter to be used within a (pre-) normative purpose. Taking into consideration the acceptability of the new filter, a primary concern in its design was that the filter should be based on the: 1) commonly available data from the wind turbines (e.g., data from nacelle anemometry), allowing to avoid the installation of additional and expensive equipment as used in this project; and 2) use of auxiliary measuring systems that are expected to be installed and operating in future floating wind parks (e.g., buoys to obtain ocean data). In the next subsection, a methodology based on clustering analysis to identify patterns in the data time series is presented. The results from each cluster are then analysed and used to assess the underlying role of wave/wind induced effects in the wind turbine power performance.

It should be noted that despite the distance between the buoy (with ocean data available) and the WindFloat system, no significant differences in the ocean conditions between the two points are expected to occur. In fact, only for waves with large wavelength, wave amplitude and direction differences may be expected for both points. For most of the wave spectrum, the differences between wave amplitude and direction should not be significant.

3.1. Clustering analysis to detect typical metocean conditions

To assess the impact of the metocean conditions on the wind turbine's power performance, a clustering analysis was applied. Clustering analysis is a typical method applied to identify and divide the data according to their similarity. The objective of this exploratory data analysis tool is to have a rather small number of clusters that contain data with similar characteristics and are, at the same time, different from the data characteristics of the remaining clusters [21], [22]. The literature on this topic is extensive with several techniques and a detailed review regarding this topic can be found in [23,24].

In this study, the K-means clustering algorithm is used to arrange the input data with similar characteristics into clusters. This information will enable an understanding of the underlying role of the metocean conditions on the wind turbine nacelle movements and power performance. The *K*-means technique is a non-hierarchical clustering algorithm for grouping the data in *K* clusters, where *K* is previously defined.

The optimal number of clusters was predetermined by calculating the Calinski-Harabasz (CH) criterion [25]. This criterion enables to identify the optimal number of clusters by computing the Euclidean distance between the clusters and comparing that to the internal sum of squared errors for each cluster. Before the clustering application, a Z-score normalization was performed for each parameter. Figure 2 depicts a flowchart of the methodology proposed to identify patterns in the data, which could be then associated with the wind turbine power performance. The metocean and wind turbine parameters used in the approach are presented in section 4.2.

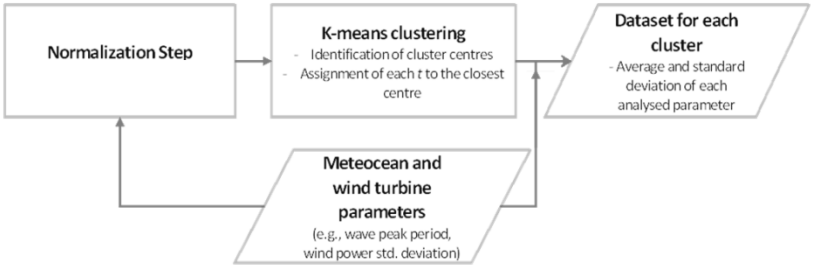

Figure 2. Flowchart of the methodology to obtain metocean patterns.

3.2. Horizontal nacelle velocity

Taking into consideration the referential defined to represent the WindFloat system movements and the load measurement system installed to monitor the wind turbine nacelle movements, the horizontal nacelle velocity (v_t) can be calculated, according to Equations (2) to (7). This parameter can then be used to understand if there is any connection between nacelle movements and the wind power, since larger movements can indicate that the turbine will not have the optimal wind area capture at all times.

(2)

$$a(t) = a_x(t) + a_y(t) + a_z(t) \tag{3}$$

$$a_x(t) = AccXC \times \cos(NacTilt) \times \cos\theta \tag{4}$$

$$a_y(t) = AccYC \times cos(NacRoll) \times cos(90 - \theta) \tag{5}$$

$$a_z(t) = \sqrt{[AccZc \times \sin(NacTilt)]^2 \times [AccZc \times \sin(NacRoll)]^2} + \cos\left[\theta - \tan^{-1}\left(\frac{-AccZc \times \sin(NacRoll)}{AccZc \times \sin(NacTilt)}\right)\right] \tag{6}$$

$$\theta = \beta - yaw_{position} \tag{7}$$

where, $a(t)$ is the total nacelle acceleration, $AccXC$ is the acceleration in x-direction of the nacelle centre of frame, $AccYC$ is the acceleration in y-direction of the nacelle centre of frame, $AccZC$ is the acceleration in z-direction of the nacelle centre of frame, *NacTilt* is the inclination sensor (tilt), *NacRoll* is the inclination sensor (roll), θ is the wind speed direction in respect to the X-direction, β is the wind direction based on the anemometry sensors and $yaw_{position}$ is the wind turbine yaw position. Due to confidential restrictions, no detailed information regarding each parameter can be presented.

The intrinsic characteristic of accelerometer sensors requires the application of a high pass frequency filter into the data gathered with a 50 Hz sampling rate. A linear trend of the total nacelle acceleration computed was removed before the numerical integration to obtain the horizontal nacelle velocity. If the acceleration signal from a real accelerometer was integrated without any filtering implemented, the results could become unbounded over time [26]. In order to obtain results with high accuracy, the numerical integration method was based on the adaptive Simpson quadrature approach with the data fitted into a polynomial function. This step was performed using the Matlab software [27].

3.3. Wind turbine power performance characterization

To understand the impact of the application of the floating offshore filter, the wind turbine's power performance characterization according to IEC 61400-12-2 [20] was performed. This standard enables the use of the nacelle anemometry to establish the wind turbine power curve, after applying a nacelle transfer function (NTF). The NTF intends to capture the turbine distortion effect on the wind speed data, and can be obtained from: 1) the turbine manufacturer, or 2) through an experimental campaign using Equation (8).

$$V_{free} = \frac{V_{free,i+1} - V_{free,i}}{V_{nacelle,i+1} - V_{nacelle,i}} \times \left(V_{nacelle} - V_{nacelle,i+1}\right) + V_{free,i} \quad (8)$$

where $V_{free,i+1}$and $V_{free,i}$ are the bin averages of the wind speed observed in the nacelle-mounted LIDAR for the wind speed bins *i+1* and *i*, respectively. The nacelle-mounted LIDAR wind speed data at 2.5D (D is rotor diameter) were used. $V_{nacelle,i+1}$ and $V_{nacelle,i}$ are the bin averages of the wind speed observed in the nacelle anemometer for the wind speed bins *i+1* and *i*, respective; and $V_{nacelle}$ is the 10-minute average observed in the nacelle anemometer. Due to the specification of the measuring systems available, it was used in this work the nacelle LIDAR instead of a traditional meteorological mast. Further details of the application of the NTF are available in [1].

4. Results

4.1. Horizontal nacelle velocity

Histogram plots for the a) 10-minute average nacelle velocity; and b) nacelle velocity standard deviation are depicted in Figure 3.

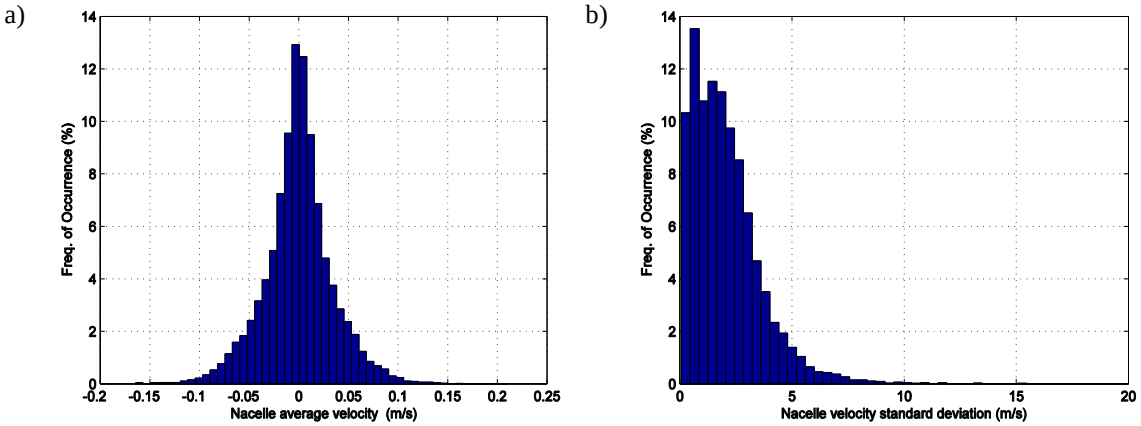

Figure 3. Histogram plot from: a) nacelle average velocity; and b) nacelle velocity standard deviation.

The results from Figure 3a) show that the nacelle average velocity - presents a normal distribution with an average value near zero, as expected due to the stability of the platform. However, within this interval, some fluctuations from the mean value were observed as can be observed in the nacelle velocity standard deviation, Figure 3b). Therefore, it is important to understand if these fluctuations within the 10-minutes average values can have impact on wind turbine power performance.

Taking into account the previous results and the data available, a new parameter - oscillation threshold (hereafter designated as threshold) - was established to assess if the horizontal nacelle velocity standard deviation - $\sigma_v(t)$ (Equation (9)) - is considerably larger than the horizontal wind speed observed in the wind turbine (data from the nacelle anemometry sensors) - $u(t)$.

$$Threshold(t) = \frac{\sigma_v(t)}{u(t)} \quad (9)$$

4.2. Detecting the impact of wave and wind in the WindFloat wind turbine

To assess the impact of the ocean conditions on the wind turbine power performance a clustering analysis using the significant wave height and wave peak period was performed in a first step. In a

second step, the clustering approach was fed with the following data: significant wave height, wave peak period, *threshold* and wind power standard deviation.

4.2.1. Clustering approach using only ocean data

According to the CH criterion, the optimal number of clusters is six, i.e., based on the selected ocean data parameters the CH criterion allows to identify six groups with similar features that are at the same time dissimilar from the remaining groups, Figure 4 - Figure 13. Figure 14 depicts the frequency of occurrence of each cluster.

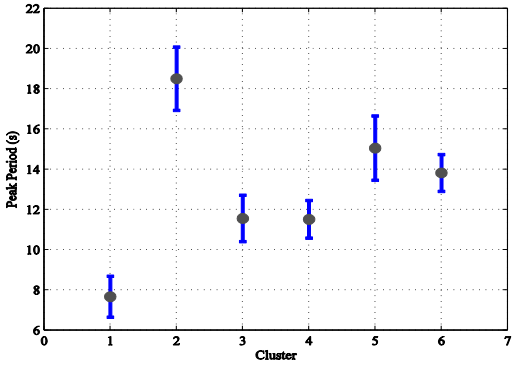

Figure 4. Wave peak period for each cluster.

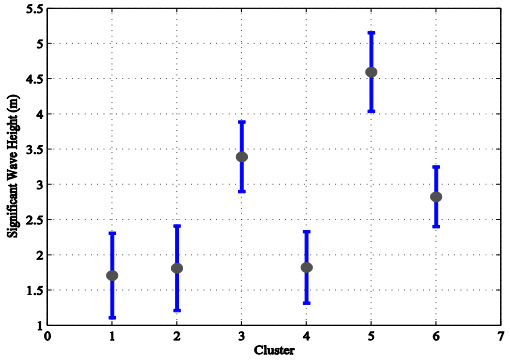

Figure 5. Significant wave height for each cluster.

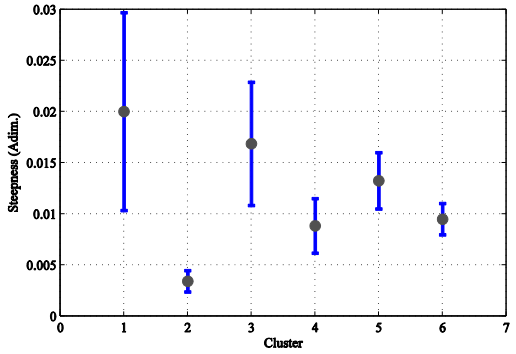

Figure 6. Wave steepness for each cluster.

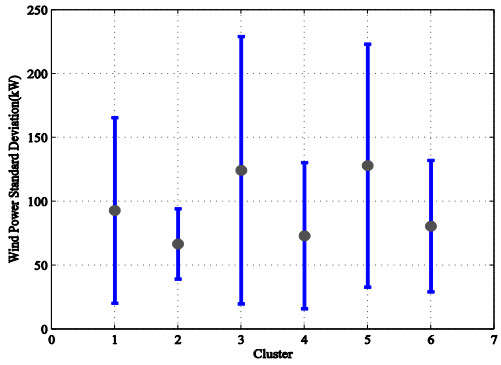

Figure 7. Wind power standard deviation for each cluster.

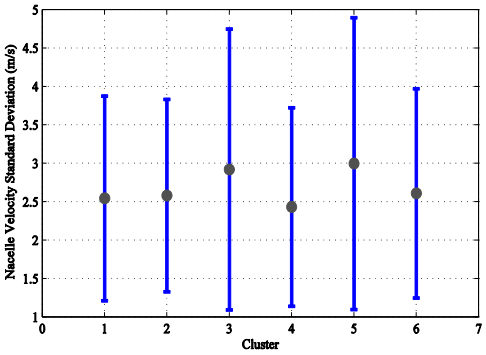

Figure 8. Nacelle velocity standard deviation for each cluster.

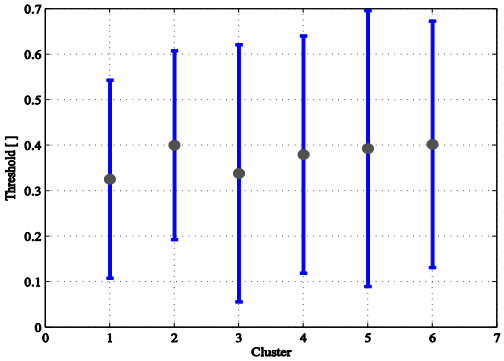

Figure 9. Threshold for each cluster.

The optimal number of clusters was predetermined by calculating the Calinski-Harabasz (CH) criterion [25]. This criterion enables to identify the optimal number of clusters by computing the Euclidean distance between the clusters and comparing that to the internal sum of squared errors for each cluster. Before the clustering application, a Z-score normalization was performed for each parameter. Figure 2 depicts a flowchart of the methodology proposed to identify patterns in the data, which could be then associated with the wind turbine power performance. The metocean and wind turbine parameters used in the approach are presented in section 4.2.

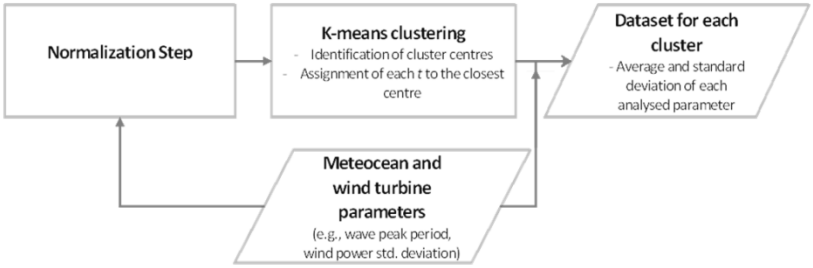

Figure 2. Flowchart of the methodology to obtain metocean patterns.

3.2. Horizontal nacelle velocity

Taking into consideration the referential defined to represent the WindFloat system movements and the load measurement system installed to monitor the wind turbine nacelle movements, the horizontal nacelle velocity (v_t) can be calculated, according to Equations (2) to (7). This parameter can then be used to understand if there is any connection between nacelle movements and the wind power, since larger movements can indicate that the turbine will not have the optimal wind area capture at all times.

(2)

$$a(t) = a_x(t) + a_y(t) + a_z(t) \quad (3)$$

$$a_x(t) = AccXC \times \cos(NacTilt) \times \cos\theta \quad (4)$$

$$a_y(t) = AccYC \times cos(NacRoll) \times cos(90 - \theta) \quad (5)$$

$$a_z(t) = \sqrt{[AccZc \times \sin(NacTilt)]^2 \times [AccZc \times \sin(NacRoll)]^2} + \cos\left[\theta - \tan^{-1}\left(\frac{-AccZc \times \sin(NacRoll)}{AccZc \times \sin(NacTilt)}\right)\right] \quad (6)$$

$$\theta = \beta - yaw_{position} \quad (7)$$

where, $a(t)$ is the total nacelle acceleration, $AccXC$ is the acceleration in x-direction of the nacelle centre of frame, $AccYC$ is the acceleration in y-direction of the nacelle centre of frame, $AccZC$ is the acceleration in z-direction of the nacelle centre of frame, *NacTilt* is the inclination sensor (tilt), *NacRoll* is the inclination sensor (roll), θ is the wind speed direction in respect to the X-direction, β is the wind direction based on the anemometry sensors and $yaw_{position}$ is the wind turbine yaw position. Due to confidential restrictions, no detailed information regarding each parameter can be presented.

The intrinsic characteristic of accelerometer sensors requires the application of a high pass frequency filter into the data gathered with a 50 Hz sampling rate. A linear trend of the total nacelle acceleration computed was removed before the numerical integration to obtain the horizontal nacelle velocity. If the acceleration signal from a real accelerometer was integrated without any filtering implemented, the results could become unbounded over time [26]. In order to obtain results with high accuracy, the numerical integration method was based on the adaptive Simpson quadrature approach with the data fitted into a polynomial function. This step was performed using the Matlab software [27].

does not demonstrate a strong association with the ocean conditions, one determines the results from wind power standard deviation observed in the cluster #1, #3 and #5 (Figure 7) are mostly controlled by the wind conditions.

4.2.2. Clustering approach using metocean and wind turbine data

According to the CH criterion, the optimal number of clusters is seven. In Figure 15 to Figure 24 the results for the different parameters are depicted. In these figures, the grey point represents the average value. In Figure 25 is depicted the frequency of occurrence of each cluster.

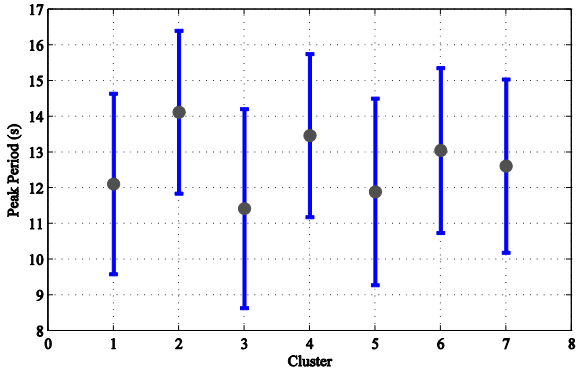

Figure 15. Wave peak period for each cluster.

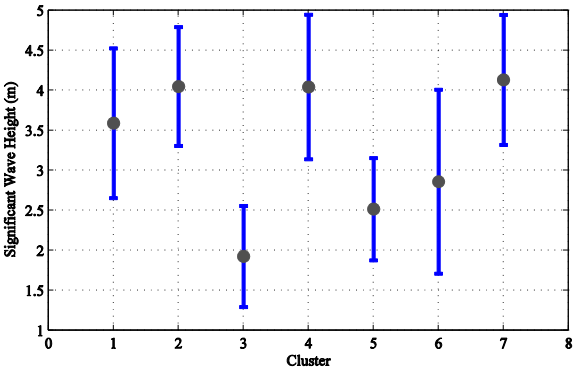

Figure 16. Significant wave height for each cluster.

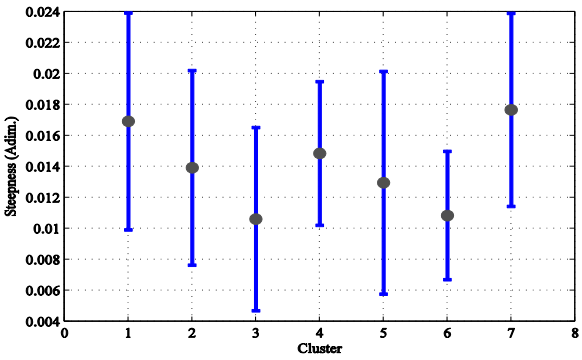

Figure 17. Wave steepness for each cluster.

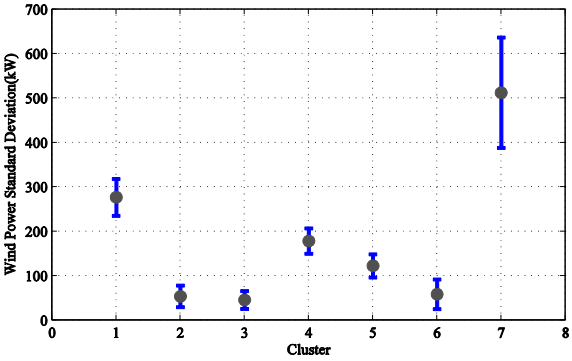

Figure 18. Wind power standard deviation for each cluster.

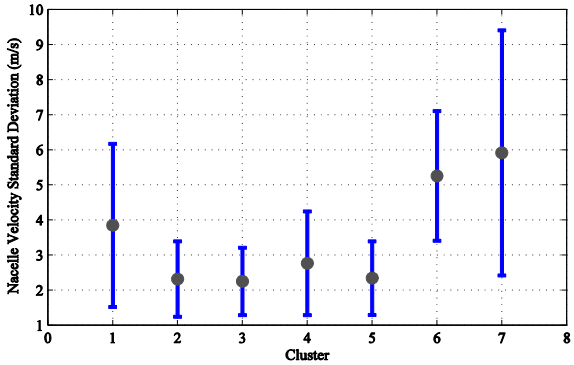

Figure 19. Nacelle velocity standard deviation for each cluster.

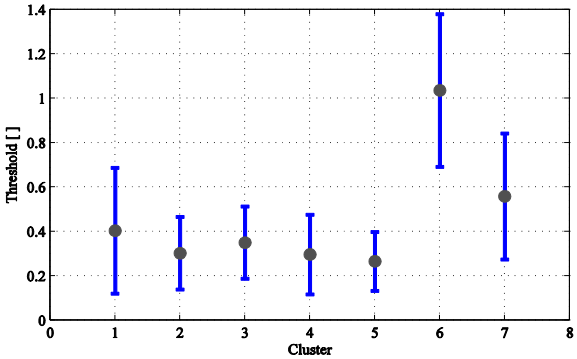

Figure 20. Threshold for each cluster.

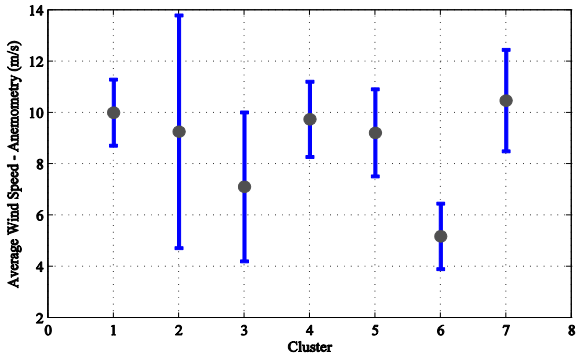

Figure 21. Average wind speed for the nacelle anemometry data for each cluster.

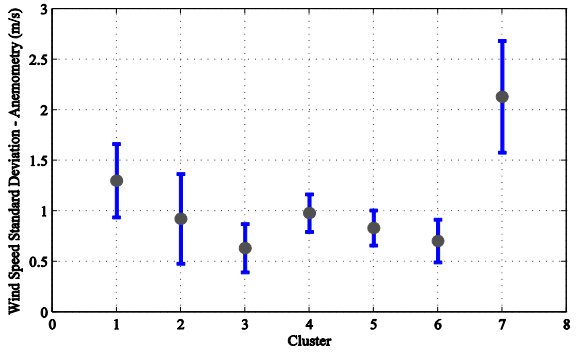

Figure 22. Wind speed standard deviation for the nacelle anemometry data for each cluster.

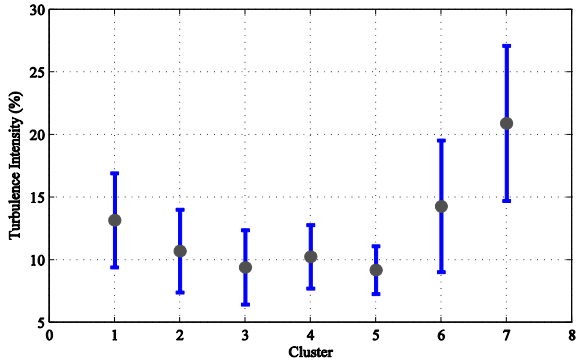

Figure 23. Turbulence intensity for the nacelle anemometry data for each cluster.

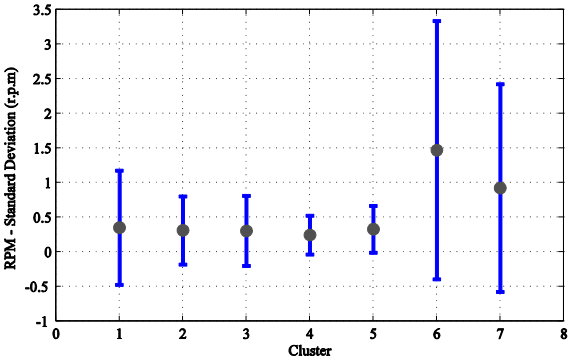

Figure 24. RPM standard deviation for each cluster.

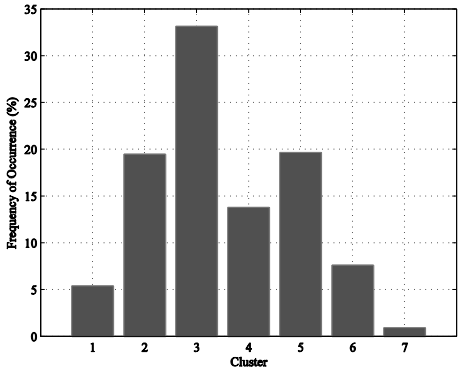

Figure 25. Frequency of occurrence of each cluster.

Again, the results demonstrate that there is no pronounced relationship between wind power standard deviation and the significant wave height or even with the wave peak period. It is not possible to associate the behaviour of the ocean parameters with the results obtained regarding the turbine power deviation/fluctuation or any other parameter that may be related to oscillations in the wind turbine nacelle. Nevertheless, and despite showing large deviations values in the standard deviation, the average wave steepness clusters present a similar behaviour when compared with the wind power standard deviation clusters.

When applying the clustering approach is possible to obtain well-defined clusters for the most relevant parameters that can affect the expected wind power production. The largest average wind power standard deviation (Figure 18) was found in cluster #7. For this cluster other parameters also show the highest average values, namely: 1) the average nacelle velocity standard deviation; 2) the turbulence intensity; 3) wave steepness; and 4) both, the average wind speed and standard deviation in the nacelle anemometry. A similar behaviour was observed for cluster #1, although with less intensity. For these two situations, the significant wave height and the wave peak period do not show a distinctive pattern

when compared with the remaining clusters. Thus, although the maritime conditions may have an impact on the expected wind power, the major influence in the fluctuations observed is driven by the atmospheric conditions. Cluster 6 helps to support that, the sea state conditions have little influence on the oscillations observed in the nacelle and in the wind power standard deviation. In this cluster, the values of standard deviation of the nacelle velocity are high. However, the wave steepness values are reduced opposing with the values observed in clusters #1 and #7 and, at the same time, the ocean conditions do not show a distinctive pattern. The values of wind power standard deviation are reduced on average, but probably due to the region of the power curve that can mitigate the possible impact of the oscillations in the wind power production. The *Threshold* parameter shows the highest value for this cluster when compared to the other groups. Considering the meaning of the parameter, it can be concluded that the nacelle velocity standard deviation is considerably larger than the horizontal wind speed observed in the wind turbine.

Taking into account Figure 20 (*threshold* values), the larger movements in the nacelle wind turbine are expected for low wind speed values and for some high wind speed situations. This fact seems to be related to the RPM standard deviation, Figure 24. These results suggest that the dynamic adaptation of the drive train system (composed of the hub, main shaft, gearbox, elastic generator coupling, bedplate and the generator) to a fast oscillating (primary energy) moving force is the source of the largest oscillations in the WindFloat wind turbine's nacelle.

The remaining groups (#2, #3, #4 and #5) show slightly different features in each cluster, namely in the height of significant waves and in the average wind speed, but overall the behaviour among themselves are quite similar. From these groups, it is possible to verify that for the majority of wind speeds no significant behaviour in the nacelle speed standard deviation is detected, or even in other parameters analysed in this study.

A relevant aspect is the statistical representability of each cluster, Figure 25. Based on the results above, the clusters that may have more impact on the power curve performance (cluster 1, cluster 6 and cluster 7) represent less than 15% of the total data. In fact, cluster #7, which shows the highest wind power deviation values, only represents around 2% of the data, followed by the cluster #1 (about 5%). Thus, the results show that for WindFloat system the wave/wind induced effects on the wind turbine power curve are reduced, and that is to be related with the wind conditions and the interaction with the wind turbine's control system. In fact, these results are in line with the results obtained in wave tank for this system [5,8,16]. Nevertheless, more studies with other parameters (*e.g.*, blade pitch as in [8]) are needed to confirm the previous results since the available dataset is quite reduced and some clusters present high values of the standard deviation in several parameters.

The previous outcomes (obtained in a real operating environment), are extremely important to demonstrate the stability of the WindFloat system, and consequently are also important for the development of the wind offshore floating industry. In fact, the non-dependency on the ocean conditions observed in this system, is contrary to the ones observed on a tension-leg platform [9].

As a final remark of these results, it should be noted that the analysis was mainly focused on the wind power standard deviation due to: 1) the WindFloat intrinsic system dynamic stability; and 2) the statistical power smoothing effect that smooths the fast power fluctuations within 10 minutes average as gathered in measurement systems available within this project (except the accelerometer data).

4.3. Floating offshore filter

Based on the results presented in the previous subsection and the sensitivity tests performed, the floating offshore filter proposed is presented in Table 2.

Table 2. Wind turbine operating range due to the floating offshore filter.

Parameter	Condition
Turbulence Intensity	[0% 12 %]
Wind speed standard deviation (nacelle anemometer sensor)	[0 1.5]

The parameters presented in Table 2 were identified as those with potentially more impact on the power performance of a floating wind turbine, which at the same time allow ingesting the impact of other experimental parameters available during the DEMOWFloat project (*e.g.*, the horizontal nacelle velocity based on accelerometer sensors).

4.4. Impact of the floating offshore filter

Two different case studies are analysed according to the filters used during the power performance characterization. According to the IEC 61400-12-2, this characterization can only occur during normal operating conditions of the wind turbine, otherwise, these periods should be excluded. In case study 1a - all filters, except the offshore floating filter, were used; case study 1b - all filters were applied filtering non-ideal operation conditions (see Table 2), which can affect the wind turbine power performance. Figure 26 and Figure 27 show the wind power curves and the standard uncertainties for the two case studies, respectively.

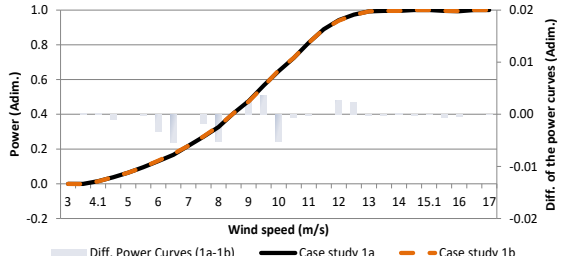

Figure 26. Wind power curves for case study 1a (black line), case study 1b (orange dashed line). The bar plot represents the difference in the power curves of each case study.

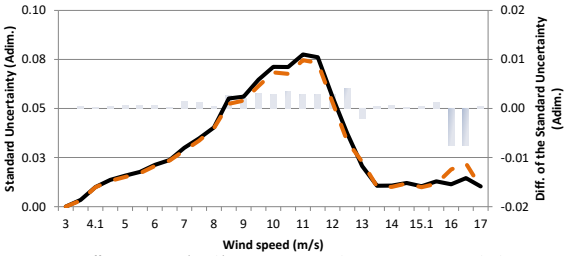

Figure 27. Standard uncertainty for case study 1a (black line), case study 1b (orange dashed line). The bar plot represents the difference in the standard uncertainties between each case study.

Results indicate that offshore floating filter (case study 1b) enables to decrease the deviation from the contracted power curve. A decrease in the standard uncertainties is also observed, Figure 27. Those results are more pronounced in the cubic zone of the wind turbine power curve, which can be explained by the elimination of some outliers detected in the wind power production by the offshore floating filter. It should be noted, that even not considering the offshore floating filter (case study 1a), the results show that the wave/wind effect impacts on the WindFloat system power performance are very reduced.

5. Conclusions

In this work, a methodology to assess the impact of the wave/wind induced oscillations on the power performance of the wind turbine operating at WindFloat floating system was presented. The methodology is based on a clustering approach and it was applied using real data. The WindFloat wind turbine nacelle movements were monitored using accelerometer sensors synchronized with the: 1) metocean data measured with a buoy; 2) wind turbine power data installed in the WindFloat floating system; and 3) wind speed data gathered from a nacelle-mounted LiDAR. To support this assessment, namely, the power performance characterization of the wind turbine according with, the existing international standards (e.g., IEC 61400-12-2) were used and adapted, when needed.

No meaningful relationship between the ocean parameters used as input (significant wave height and wave peak period) and the nacelle movements or the wind power (standard deviation) production could be established. Results suggest that the dynamic adaptation of the wind turbine drive train to fast fluctuations on the wind speed is the source of the largest oscillations in the WindFloat wind turbine nacelle.

The application of the offshore floating filter (case study 1b) presented in this work enabled to remove non-typical operation conditions reducing the deviation from the contracted power curve, and also decreasing the standard uncertainties. The application of the filter enables to observe that the oscillations have a reduced impact on the power performance of the wind turbine and it is explained

by the high dynamic stability of the WindFloat platform. Therefore, it is recommended that future works include this parameter as a filter during the power performance procedures of floating wind turbines. It is also recommended for future studies the deployment of the measuring systems i) as close as possible to minimize the impact of a possible time gap between the wave measurement location and the floating system and ii) capable of collecting data with a high-frequency rate.
The previous results, obtained in a real operating environment, were instrumental to prove the stability of the WindFloat system, enabling this concept to reach the commercial phase. In fact, the first wind park (with nearly 25 MW) based on this concept was deployed in Portugal in 2020 and further floating offshore wind parks are already foreseen in the next years.

6. References

[1] European Commission 2020 An EU Strategy to harness the potential of offshore renewable energy for a climate neutral future {SWD(2020) 273 final} EN *SWD(2020) 273 Final* 27
[2] Jiang Z 2021 Installation of offshore wind turbines: A technical review *Renew. Sustain. Energy Rev.* **139** 110576
[3] Chitteth Ramachandran R, Desmond C, Judge F, Serraris J-J and Murphy J 2021 Floating offshore wind turbines: Installation, operation, maintenance and decommissioning challenges and opportunities *Wind Energy Sci. Discuss.* 32
[4] Wen B, Li Z, Jiang Z, Tian X, Dong X and Peng Z 2022 Floating wind turbine power performance incorporating equivalent turbulence intensity induced by floater oscillations *Wind Energy* **25** 260–80
[5] Roddier D, Cermelli C, Aubault A and Weinstein A 2010 WindFloat: A floating foundation for offshore wind turbines *J. Renew. Sustain. Energy* **2** 1–34
[6] Urbán A M and Guanche R 2019 Wind turbine aerodynamics scale-modeling for floating offshore wind platform testing *J. Wind Eng. Ind. Aerodyn.* **186** 49–57
[7] Failla G and Arena F 2015 New perspectives in offshore wind energy *Philos Trans A Math Phys Eng Sc.* **373** 13
[8] Cermelli C, Roddier D and Aubault A 2009 WINDFLOAT: A Floating Foundation For Offshore Wind Turbines Part II: Hydrodynamics Analysis *Proceedings of the ASME 28th International Conference on Ocean, Offshore and Arctic Engineering, OAME2009* (Hawaii (USA)) pp 1–9
[9] Sant T, Bonnici D, Farrugia R and Micallef D 2015 Measurements and modelling of the power performance of amodel floating wind turbine under controlled conditions *Wind Energy* **18** 811–34
[10] Rockel S, Peinke J, Hölling M and Cal R B 2016 Wake to wake interaction of floating wind turbine models in free pitch motion: An eddy viscosity and mixing length approach *Renew. Energy* **85** 666–76
[11] Farrugia R, Sant T and Micallef D 2016 A study on the aerodynamics of a floating wind turbine rotor *Renew. Energy* **86** 770–84
[12] Chen P, Chen J and Hu Z 2020 Review of Experimental-Numerical Methodologies and Challenges for Floating Offshore Wind Turbines *J. Mar. Sci. Appl.* **19** 339–61
[13] Tran T-T and Kim D-H 2015 The platform pitching motion of floating offshore wind turbine: A preliminary unsteady aerodynamic analysis *J. Wind Eng. Ind. Aerodyn.* **142** 65–81
[14] Lei H, Zhou D, Lu J, Chen C, Han Z and Bao Y 2017 The impact of pitch motion of a platform on the aerodynamic performance of a floating vertical axis wind turbine *Energy* **119** 369–83
[15] Wen B, Dong X, Tian X, Peng Z, Zhang W and Wei K 2018 The power performance of an offshore floating wind turbine in platform pitching motion *Energy* **154** 508–21
[16] Nejad A R and Torsvik J 2021 Drivetrains on floating offshore wind turbines: lessons learned over the last 10 years *Forsch. im Ingenieurwes.* **85** 335–43
[17] Johlas H M, Martínez-Tossas L A, Churchfield M J, Lackner M A and Schmidt D P 2021 Floating platform effects on power generation in spar and semisubmersible wind turbines *Wind Energy* **24** 901–16
[18] Roddier D, Cermelli C and Weinstein A 2009 WINDFLOAT: A Floating Foundation For Offshore Wind Turbines Part I: Design Basis And Qualification Process *Proceedings of the ASME 28th International Conference on Ocean, Offshore and Arctic Engineering, OAME2009* (Hawaii (USA)) pp 1–9
[19] Santos C Commercial Floating Wind The WindFloat role *Business2Sea - Ocean Obs. Mar. Technol.* 13
[20] International Electrotechnical Commission 2013 *Wind turbines - Part 12-2: Power performance of electricity-producing wind turbines based on nacelle anemometry (Ed. 1)*
[21] Yarnal B, Comrie A C, Frakes B and Brown D P 2001 Review developments and prospects in synoptic climatology *Int. J. Climatol. (Special Rev. Issue)* **21** 1923–50
[22] Couto A, Costa P, Rodrigues L, Lopes V V. and Estanqueiro A 2015 Impact of Weather Regimes on the Wind Power Ramp Forecast in Portugal *IEEE Trans. Sustain. Energy* **6** 934–42

[23] Huth R, Beck C, Philipp A, Demuzere M, Ustrnul Z, Cahynová M, Kyselý J and Tveito O E 2008 Classifications of atmospheric circulation patterns: recent advances and applications. *Ann. N. Y. Acad. Sci.* **1146** 105–52
[24] Lloyd S 1982 Least squares quantization in PCM *IEEE Trans. Inf. Theory* **28** 129–37
[25] Calinski T and Harabasz J 1974 A dendrite method for cluster analysis *Commun. Stat. - Theory Methods* **3** 1–27
[26] Slifka L D 2004 An accelerometer based approach to measuring displacement of a vehicle body *Master thesis Univ. Michigan* 66
[27] Matlab MATLAB and Neural Network Toolbox Release 2012b, The MathWorks, Inc., Natick, Massachusetts, United States.

Acknowledgements
This work was partially funded by the European Commission FP7 project ‘‘DEMOWFLOAT – Demonstration of the WindFloat Technology’’, Grant Agreement number: ENER/FP7/296050/ DEMOWFLOAT. The authors gratefully acknowledge EDP-Inovação, Repsol and Principle Power for providing and authorizing the use of the data, processed under this work and the LNEG for co-financing and providing the conditions to conduct this research.